Solving the small-scale structure puzzles with dissipative dark matter

Robert Foot[1]

ARC Centre of Excellence for Particle Physics at the Terascale,
School of Physics, University of Melbourne,
Victoria 3010 Australia

Sunny Vagnozzi[2]

The Oskar Klein Centre for Cosmoparticle Physics,
Department of Physics, Stockholm University, AlbaNova University Center,
Roslagstullbacken 21A, SE-106 91 Stockholm, Sweden

NORDITA (Nordic Institute for Theoretical Physics),
KTH Royal Institute of Technology and Stockholm University,
Roslagstullbacken 23, SE-106 91 Stockholm, Sweden

Small-scale structure is studied in the context of dissipative dark matter, arising for instance in models with a hidden unbroken Abelian sector, so that dark matter couples to a massless dark photon. The dark sector interacts with ordinary matter via gravity and photon-dark photon kinetic mixing. Mirror dark matter is a theoretically constrained special case where all parameters are fixed except for the kinetic mixing strength, ϵ. In these models, the dark matter halo around spiral and irregular galaxies takes the form of a dissipative plasma which evolves in response to various heating and cooling processes. It has been argued previously that such dynamics can account for the inferred cored density profiles of galaxies and other related structural features. Here we focus on the apparent deficit of nearby small galaxies ("missing satellite problem"), which these dissipative models have the potential to address through small-scale power suppression by acoustic and diffusion damping. Using a variant of the extended Press-Schechter formalism, we evaluate the halo mass function for the special case of mirror dark matter. Considering a simplified model where $M_{\text{baryons}} \propto M_{\text{halo}}$, we relate the halo mass function to more directly observable quantities, and find that for $\epsilon \approx 2 \times 10^{-10}$ such a simplified description is compatible with the measured galaxy luminosity and velocity functions. On scales $M_{\text{halo}} \lesssim 10^8 \ M_\odot$, diffusion damping exponentially suppresses the halo mass function, suggesting a nonprimordial origin for dwarf spheroidal satellite galaxies, which we speculate were formed via a top-down fragmentation process as the result of nonlinear dissipative collapse of larger density perturbations. This could explain the planar orientation of satellite galaxies around Andromeda and the Milky Way.

---

[1]E-mail address: rfoot@unimelb.edu.au
[2]E-mail address: sunny.vagnozzi@fysik.su.se

1 Introduction

The ΛCDM model has been very successful in describing the large-scale structure of the Universe on cluster scales and above, and the Cosmic Microwave Background (CMB), see e.g. [1–9]. Structure forms hierarchically (bottom-up) with the smaller structures forming first eventually merging in ever-growing larger structures. In this picture, dark matter (DM) is presumed to be composed of massive collisionless particles influenced only by gravity with no other (astrophysically significant) forces. On smaller scales, though, there are indications that something might be lacking in this description. For instance, the density profile of galaxies (in particular dwarf galaxies) is known to deviate from the cuspy profile predicted from collisionless cold dark matter (CDM hereafter) only simulations, an issue which is known as the "core-cusp problem" (see e.g. [10] for a recent review). In addition, the number of nearby small galaxies is found to be much lower than expected if DM is both cold and collisionless. This problem is most severe for small satellite galaxies ("missing satellite problem") [11, 12], but also exists for field galaxies, see e.g. [13–15]. The issue is actually more acute than simply being a local problem, as the observed luminosity and HI mass functions exhibit faint-end slopes which are much shallower than those predicted by collisionless CDM [16]. See also [17, 18] for further discussions on related issues.

If one insists that dark matter is cold and collisionless then baryonic physics must ultimately resolve the small scale issues, including those identified above. This is a popular approach adopted in many studies, e.g. [19, 20]. Here we pursue a very different path. Namely that the small scale features are taken as evidence that dark matter has nontrivial self-interactions cf. [21–23]. Here we focus on a particular scenario where the DM emerges from a hidden sector with an unbroken Abelian $U(1)'$ gauge interaction. The associated massless gauge boson, called the dark photon, mediates self interactions which are also dissipative. Models of this kind have been discussed for quite some time in the literature, with mirror dark matter, where the hidden sector is exactly isomorphic to the Standard Model (SM), representing the theoretically most constrained example [23–34]. For a review and more detailed bibliography see e.g. [35]. More generic such models have also been explored in recent years, see e.g. [36–54] for a partial bibliography. The simplest generic model consists of two massive particles, usually taken to be fermions, charged under this $U(1)'$ gauge symmetry. The dark sector interacts with the SM sector by gravity and via the photon-dark photon kinetic mixing interaction.

Such dissipative DM models can reproduce the successful large-scale structure and CMB predictions of collisionless CDM [27–29, 33, 45, 47]. The dynamics of these models on smaller scales is quite nontrivial. In the case of spiral and irregular galaxies, the physical picture consists of the DM halo taking the form of a dissipative plasma which evolves in response to various heating and cooling processes. At the present time, the halo is presumed to have (typically) reached a steady-state configuration where the energy lost due to dissipative interactions is replaced by energy produced by ordinary supernovae; the precise mechanism involves kinetic mixing-induced processes transferring core-collapse energy into dark photons. In fact, it has been argued that the nontrivial dissipative dynamics of such models can provide a dynamical explanation for the inferred cored density profile in galaxies, the Tully-Fisher relation, and some related structural issues [51, 55–58]. However, there has been significantly less work addressing other small-scale problems, including the apparent deficit of small galaxies. It has been known for some time that dissipative DM features suppressed power on small scales due to dark acoustic oscillations and dark photon diffusion, and therefore has the potential

to address this important problem.

Structure formation with suppressed small-scale power has recently been studied in [59–61]. It was shown that the extended Press-Schechter (EPS) approach [62, 63], implemented with a sharp-k filter, leads to good agreement with simulations. In this paper we apply this formalism to the specific case of dissipative DM to estimate the halo mass function. This gives us the number density per unit mass of collapsed objects (dark halos) in the Universe. To make contact with observations, we still need to relate the halo mass to some directly measurable quantity, such as luminosity or rotational velocity. It would be helpful if we knew the ratio of baryons to dark matter in a given galaxy, but even that can be difficult to determine. Although cosmology gives us the baryonic mass fraction in the Universe (that is, $\Omega_b/\Omega_m \simeq 0.15$), on small scales, i.e. within galaxies, baryonic effects such as photoionization and/or supernova feedback (e.g. [64]) can potentially cause departures from this cosmic value. The size of these baryonic effects are, of course, quite uncertain and indications that these effects may not be so significant persist (see e.g. [16] and references therein). Thus, as a simplified model we consider $M_b \propto M_{\rm halo}$ with the proportionality factor tentatively set to $\Omega_b/\Omega_m \approx 0.15$. While somewhat smaller values are preferred by various constraints such as weak lensing and satellite kinematics (e.g. [65, 66]), variation of the $M_b/M_{\rm halo}$ ratio by a factor of 2 or 3 does not affect our conclusions.

This paper is structured as follows. In Section 2, we briefly review some aspects of the hidden sector $U(1)'$ framework, defining the prototype dissipative DM model. In Section 3, we consider the matter power spectrum, compute it for some illustrative examples, and briefly discuss the relevant physical processes affecting the growth of structure: acoustic damping and diffusion damping. In Section 4 we give our results for the halo mass function which we compare with observations using our simplified $M_b \propto M_{\rm halo}$ assumption. We also make a few speculations regarding the origin of the dwarf spheroidal satellites in the Milky Way and Andromeda systems. Our conclusions are given in Section 5.

2   Dissipative hidden sector dark matter

The prototype model for dissipative dark matter presumes the existence of a hidden sector with an unbroken $U(1)'$ gauge interaction. The DM then consists of particles carrying $U(1)'$ charge, with the minimal case having two such particles, a "dark electron" (e_d) and a "dark proton" (p_d). The fundamental interactions are described by the following Lagrangian:

$$\mathcal{L} = \mathcal{L}_{SM} \quad -\frac{1}{4}F'^{\mu\nu}F'_{\mu\nu} + \bar{e}_d(iD_\mu\gamma^\mu - m_{e_d})e_d + \bar{p}_d(iD_\mu\gamma^\mu - m_{p_d})p_d + \mathcal{L}_{\rm mix} \qquad (1)$$

where $\mathcal{L}_{SM}$ denotes the $SU(3)_c \otimes SU(2)_L \otimes U(1)_Y$ gauge invariant Standard Model Lagrangian which describes the interactions of the SM particles. Also, $F'_{\mu\nu} = \partial_\mu A'_\nu - \partial_\nu A'_\mu$ [$B_{\mu\nu} = \partial_\mu B_\nu - \partial_\nu B_\mu$] is the field strength tensor associated with the $U(1)'$ [$U(1)_Y$] gauge interaction, A'_μ [$B_\mu = \cos\theta_w A_\mu + \sin\theta_w Z_\mu$] being the relevant gauge field. The two dark fermions are described by the quantum fields e_d, p_d and the covariant derivative is: $D_\mu = \partial_\mu + ig'Q'A'_\mu$ (where g' is the coupling constant relevant to this gauge interaction). While we assume that the dark electron and dark proton have $U(1)'$ charges opposite in sign, we make no assumption about their relative magnitude (that is, the ratio $|Q'(p_d)/Q'(e_d)|$ defines a fundamental parameter of the theory). The self-interactions of the dark electron can be defined in terms of the dark fine structure

constant, $\alpha_d \equiv [g'Q'(e_d)]^2/4\pi$. The relic abundance of dark electrons and dark protons is presumed to be set by a particle-antiparticle asymmetry (that is, the relic abundance of dark antielectrons and dark antiprotons is negligible). For further discussions of such asymmetric DM models, including possible mechanisms for generating the required asymmetry, see e.g. [67,68].

In addition to gravity, the dark sector interacts with the SM particles via the kinetic mixing interaction between the dark photon and the hypercharge gauge boson [26,69]:

$$\mathcal{L}_{\text{mix}} = \frac{\epsilon'}{2} \, B^{\mu\nu} F'_{\mu\nu} \ . \tag{2}$$

This renormalizable and gauge-invariant interaction also leads to photon - dark photon kinetic mixing. The kinetic mixing interaction imbues the dark electron and dark proton with an ordinary electric charge proportional to ϵ', taken to be: ϵe and $Z'\epsilon e$, where $Z' \equiv |Q'(p_d)/Q'(e_d)|$ [70]. The new physics is then fully described by the fundamental parameters: $m_{e_d}, m_{p_d}, Z', \alpha_d$ and ϵ.

Mirror dark matter can be viewed as a special case of the above formalism. That is, mirror DM corresponds to having the dark sector described by a Lagrangian which exactly mirrors that of the SM. In this situation an exact and unbroken $\mathbb{Z}_2$ discrete symmetry can be identified. Mirror dark matter is thereby theoretically constrained, with $\alpha_d = \alpha$, $m_{e_d} = m_e$, $m_{p_d} = m_p$. Also, $Z' = 1$ for the lightest states (that theory has, of course, a spectrum of dark nuclei).

Cosmological, astrophysical, and some experimental aspects of this and related models have been explored in the literature, e.g. [25, 27–29, 33, 35, 36, 39–41, 43–54, 71–77]. Regarding the Early Universe, the thermodynamics of the SM and DM systems can each be described with a temperature which needs not be the same for each sector. Define T_γ [T_{γ_D}] to be the photon [dark photon] temperature, then Big Bang Nucleosynthesis and CMB considerations typically constrain the energy density of any exotic radiation component: $(T_{\gamma_D}/T_\gamma)^3 \ll 1$. Such considerations will therefore also lead to constraints on the kinetic mixing parameter, ϵ, since kinetic mixing induced processes such as $\bar{e}e \to \bar{e}_d e_d$ will transfer entropy to the dark sector. That is, even if we started with an effective initial condition, $T_{\gamma_D}/T_\gamma \ll 1$, kinetic mixing induced processes can potentially thermalize the SM and dark sectors [evolve $T_{\gamma_D}/T_\gamma \to 1$] and thereby violate the constraints on additional energy density. For $m_{e_d} \sim$ MeV, the relevant constraint is: $\epsilon \lesssim 3 \times 10^{-9}$ [51, 72, 73].

Kinetic mixing processes can only be effective for temperatures, $T \gtrsim \mathcal{M}$, where $\mathcal{M} \equiv \max(m_e, m_{e_d})$. Below this temperature, these processes cease to be important and the ratio T_{γ_D}/T_γ stabilizes. This asymptotic value for T_{γ_D}/T_γ was found to satisfy [51]:

$$x \equiv \frac{T_{\gamma_D}}{T_\gamma} \ \simeq \ 0.31 \sqrt{\frac{\epsilon}{10^{-9}}} \left(\frac{m_e}{\mathcal{M}}\right)^{\frac{1}{4}} \ , \tag{3}$$

for parameters in the range $\epsilon \lesssim$ few $\times 10^{-9}$ and 0.1 MeV $\lesssim m_{e_d} \lesssim$ 100 MeV.

There is an additional source of constraints arising from Early Universe cosmology. Prior to dark recombination, the dark electrons and dark protons are strongly coupled to each other and to the dark photons, behaving as a tightly coupled fluid. Due to the large restoring force from the dark radiation pressure this fluid undergoes acoustic oscillations which inhibit the formation of structure on scales smaller than the sound horizon at dark recombination. Too much suppression of structure on scales which are growing linearly today can be excluded from observations, leading to the rough bound

3

(e.g. [51, 67, 77]):

$$\epsilon \lesssim 10^{-8} \left(\frac{\alpha_d}{\alpha}\right)^4 \left(\frac{m_{e_d}}{\text{MeV}}\right)^2 \left(\frac{\mathcal{M}}{m_e}\right)^{\frac{1}{2}} . \tag{4}$$

However, some suppression of small-scale power is desirable. Indeed acoustic oscillations, as well as damping due to dark photon diffusion, might be the physical mechanisms responsible for the observed suppression of the number of small galaxies relative to expectations from collisionless CDM.

3 Matter power spectrum

It has been known for some time that this kind of dissipative DM reproduces collisionless CDM on large scales with deviations on small scales. The deviations arise from two effects: acoustic oscillations and dark photon diffusion. Both effects operate before and during dark recombination, and can be characterized by physical scales which depend on the fundamental parameters.

The effects can be described by two-point correlation functions of the density field fluctuations, such as the matter power spectrum. This quantity is straightforward to compute, and we will need it later on in order to estimate the halo mass function via the extended Press-Schechter formalism. If we define the mass density as $\rho(\mathbf{x})$, then inhomogeneities can be described by: $\delta(\mathbf{x}) \equiv [\rho(\mathbf{x}) - \rho_M]/\rho_M$ where ρ_M is the mean mass density in the Universe. The power spectrum is related to the Fourier transform of this fractional overdensity, $\delta(\mathbf{k})$, by:

$$\langle \delta(\mathbf{k}) \delta^\star(\mathbf{k}') \rangle = (2\pi)^3 P(k) \delta^3(\mathbf{k} - \mathbf{k}') , \tag{5}$$

where the brackets indicate an ensemble average. In practice, the linear power spectrum is determined by solving the set of coupled Boltzmann equations for photons, baryons, neutrinos, DM and dark radiation. Since dissipative DM shares many similarities with SM baryons, the appropriate Boltzmann equations are straightforward generalizations of those for photons and baryons. For the special case of mirror DM they are given in [33] and they may be easily adapted to the general case.

For our numerical work, we consider a flat Universe with parameters: $\Omega_b = 0.022 \, h^{-2}$, $\Omega_{\rm dm} = 0.12 \, h^{-2}$, $h = 0.70$, and assume a scale-invariant Harrison-Zel'dovich-Peebles primordial power spectrum of density fluctuations (that is, the spectral index is $n_s = 1$). The effects of a small tilt, or small changes to $\Omega_b, \Omega_{\rm dm}, h$, are not important for our considerations. We also consider mirror DM parameters ($\alpha_d = \alpha$, $m_{e_d} = m_e$, $m_{p_d} = m_p$, $Z' = 1$) to illustrate the physics.[3] With these parameters fixed, our results depend only on the kinetic mixing parameter, ϵ [or equivalently, the ratio of the dark sector temperature to the visible sector temperature x, given Eq.(3)]. Figure 1 compares the matter power spectrum with $x = 0$, cosmologically equivalent to collisionless CDM, with

---

[3] The mirror DM model has a spectrum of dark "mirror nuclei" composed predominately of mirror hydrogen ($Z' = 1$, $m = m_p$) and mirror helium ($Z' = 2$, $m = 4m_p$). It follows that the chosen mirror DM parameters give results for that model only if mirror hydrogen dominates over mirror helium, i.e. the mirror helium mass fraction is zero ($Y_{He'} = 0$). However, the expectation from mirror Big Bang Nucleosynthesis is that mirror helium dominates over mirror hydrogen [27], with $Y_{He'} \approx 0.9$ for $\epsilon \sim 10^{-9}$ [78]. Nevertheless, it turns out that the matter power spectrum and baryonic mass function depend weakly on $Y_{He'}$, and we have checked (for $x = 0.15$) that the power spectrum (and mass function) results for $Y_{He'} = 0$ are in fact a good estimate for $Y_{He'} \approx 0.90$.
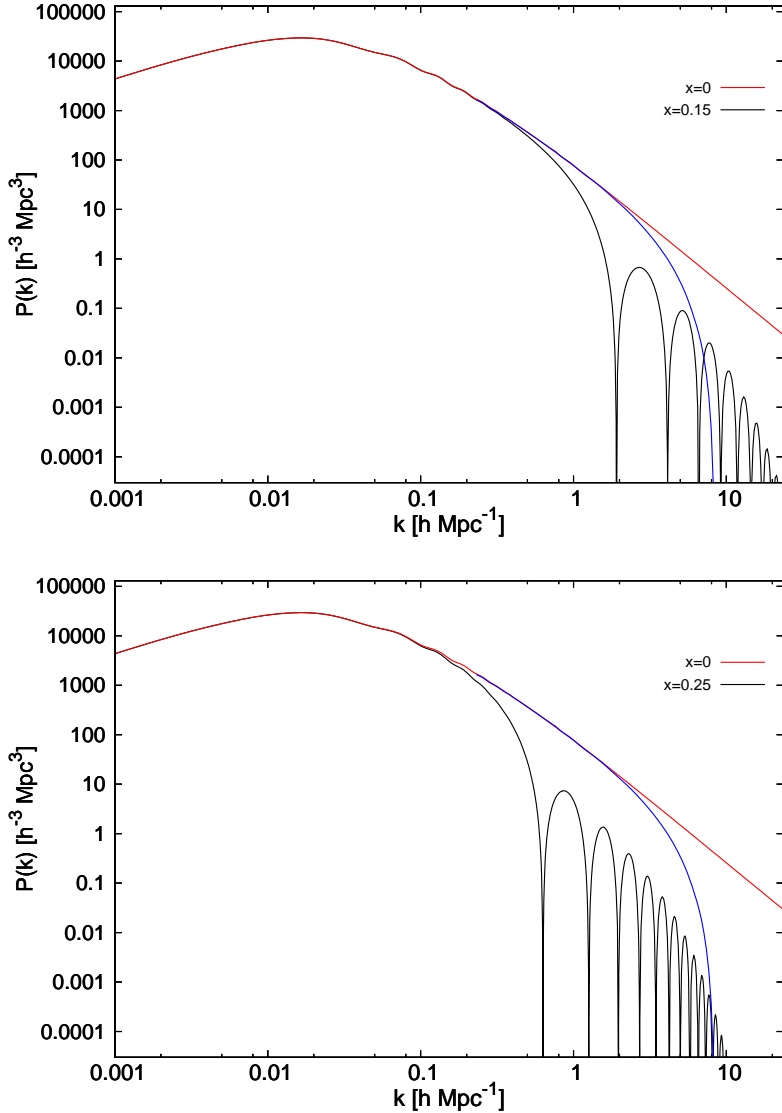
Figure 1: Matter power spectrum for mirror DM parameters with $x = 0$ (top red curves in figures) and $x = 0.15$ (black curve in Figure 1a), $x = 0.25$ (black curve in Figure 1b). These values of x correspond to $\epsilon \simeq 2.3 \times 10^{-10}$, 6.5×10^{-10} respectively, from Eq.(3). Note that the $x = 0$ curve is identical to the standard matter power spectrum for collisionless CDM. For comparison the power spectrum of a warm DM cosmology, with a thermal equivalent warm DM particle mass of 2 keV, is also shown (blue curves in the two figures).

our model for two examples. The figure shows that the model reproduces the predictions of collisionless CDM on large scales with departures on small scales.

The modifications to the power spectrum evident in the figures have been previously discussed in the literature [27–29,33,45,47]. The coupling of the DM to the thermal bath of dark radiation significantly suppresses the growth of structures on scales below the sound horizon at dark recombination. The way it does so can be understood in terms of two important effects: acoustic damping due to dark acoustic oscillations (DAOs), and diffusion damping (*collisional damping*) due to dark photon diffusion. Associated to each of these effects is a characteristic scale (length scale or, equivalently, comoving wavenumber), which can be expressed in terms of the fundamental parameters of the model. We provide an analytical estimate of these scales in Appendix A.

Acoustic damping can be understood by recalling that, prior to recombination of the dark electrons and dark protons into neutral bound states, the behaviour of the DM can be modelled as that of a tightly coupled fluid. The interplay between gravity and the corresponding restoring force determined by dark radiation pressure leads to the phenomenon of DAOs which suppresses the growth of structure on scales smaller than the size of the sound horizon at the epoch of dark recombination. This effect is analogous to the well-known baryonic acoustic oscillations (BAOs), which imprints the visible sector sound horizon scale at decoupling ($\sim 105\ h^{-1}$ Mpc) on the late-time clustering of matter.[4]

The other effect is due to the tiny but non-negligible dark photon free-streaming length at the epoch of dark recombination. Dark photon diffusion acts to erase small-scale inhomogeneities and anisotropies, below the dark photon free-streaming length. This effect is known as diffusion damping, and is analogous to its visible counterpart known as Silk damping, responsible for the suppression of the high-l acoustic peaks of the CMB angular power spectrum [83]. Diffusion damping effectively provides an exponentially damping envelope which reduces the power on scales below the dark photon mean free path at the dark recombination epoch. This effect is qualitatively similar to the small-scale power suppression in warm dark matter (WDM) models. In that case the suppression is due to *collisionless damping*: that is, free-streaming of high-velocity DM particles out of initial overdensities, leading to a sharp cut-off in power below a critical scale.

It should be possible to derive constraints on small-scale power suppression from Lyman-α forest considerations (e.g. [84–86]). In fact, it has been found that the matter power spectrum for $k \lesssim 2\ h^{-1}$ Mpc approximately agrees with that predicted by collisionless CDM (e.g. [86]). This could be used to infer a rough upper bound: $k_{\mathrm{DAO}} \gtrsim 2\ h^{-1}$ Mpc, which for mirror DM parameters [cf. with Eq.(21)] suggests $x \lesssim 0.15$. This rough bound is subject to a few important caveats. Firstly, there can be significant uncertainties when converting the Lyman-α flux power to the linear matter power spectrum [87]. Secondly, these analyses typically make simplifying assumptions on the shape of the power spectrum (power-law with a running spectral index) which could make application of these bounds to models with DAOs problematic [45]. Finally, as remarked in [50], to accurately evaluate Lyman-α forest constraints on these kinds of self-interacting DM models would ultimately require careful hydrodynamical simulations which have not yet been done.

4   Halo and baryonic mass function

Ultimately we would like to describe the structure in the Universe: the distribution of galaxies and their DM halos as a function of their masses. To this end, we need to know one-point statistics such as the halo mass function: the number density of collapsed objects per unit logarithmic mass in the Universe. The extended Press-Schechter (EPS) formalism [62, 63] is a simple analytic approach which allows us to calculate the halo mass function (for a review and more detailed bibliography, see e.g. [88]). This method assumes linear growth of perturbations and subsequent immediate halo collapse when the mass overdensity reaches a certain critical threshold (which is itself derived from an

---

[4]Dark acoustic oscillations can arise more generally in models where the DM couples to relativistic particles. Among these are models where the DM couples to neutrinos (see e.g. [79,80]), and photons (see e.g. [81,82]).

idealised spherical or ellipsoidal collapse toy model).

In the EPS formalism the halo mass function takes the form:

$$\frac{dn}{d \ln M_{\text{halo}}} = \frac{1}{2} \frac{\bar{\rho}}{M} f(\nu) \frac{d \ln \nu}{d \ln M_{\text{halo}}} \, , \tag{6}$$

where we have denoted by n the number density of collapsed objects (halos), whose mass is given by M_{halo}, $\bar{\rho}$ is the average matter density in the Universe, while the first-crossing distribution $f(\nu)$ will be defined shortly. Also, ν is defined as:

$$\nu \equiv \frac{\delta_c^2}{S(R)} \, , \tag{7}$$

where the critical overdensity for collapse at redshift 0 evaluates to $\delta_c \simeq 1.686$. In Eq.(7), $S(R)$ is the variance function of the density field smoothed over a length scale R (which corresponds to a mass scale M once a map between the two is given):

$$S(R) = \frac{1}{2\pi^2} \int dk \; k^2 P(k) |W(k;R)|^2 \, . \tag{8}$$

In Eq.(8), $P(k)$ is the linear matter power spectrum at redshift $z = 0$. Also, $W(k;R)$ is the Fourier transform of the filter function, which we will return to in a moment. Finally, the first-crossing distribution $f(\nu)$ can be obtained by utilizing the excursion-set approach, which follows random walk trajectories and counts the first up-crossings of the collapse threshold. In the case of ellipsoidal collapse, the first-crossing distribution takes the form [89]:

$$f(\nu) = A \sqrt{\frac{2q\nu}{\pi}} \left[1 + (q\nu)^{-p} \right] e^{-\frac{q\nu}{2}} \, , \tag{9}$$

where $A = 0.3222$, $p = 0.3$ and $q = 1$.

Crucial to the success of the EPS formalism is the choice of filter function $W(k;R)$. For DM models with small-scale power suppression, a sharp-k filter has been found to reproduce results of simulations [59–61]. The more common choice of real-space top-hat filter instead fails to match the simulations. The reason is readily understood upon inspection of Eq.(8): if the real-space top-hat filter is used then the variance function becomes insensitive to the power spectrum in the suppressed regime (where the power decreases more steeply than k^{-3}) as the form of the halo mass function is then driven solely by the filter function.

The sharp-k filter is a top-hat function in Fourier space: $W(k;R) \equiv \Theta(1 - kR)$, where Θ denotes the Heaviside step function. With this choice of window function, the form of the halo mass function [Eq.(6)] reduces to the simple expression:
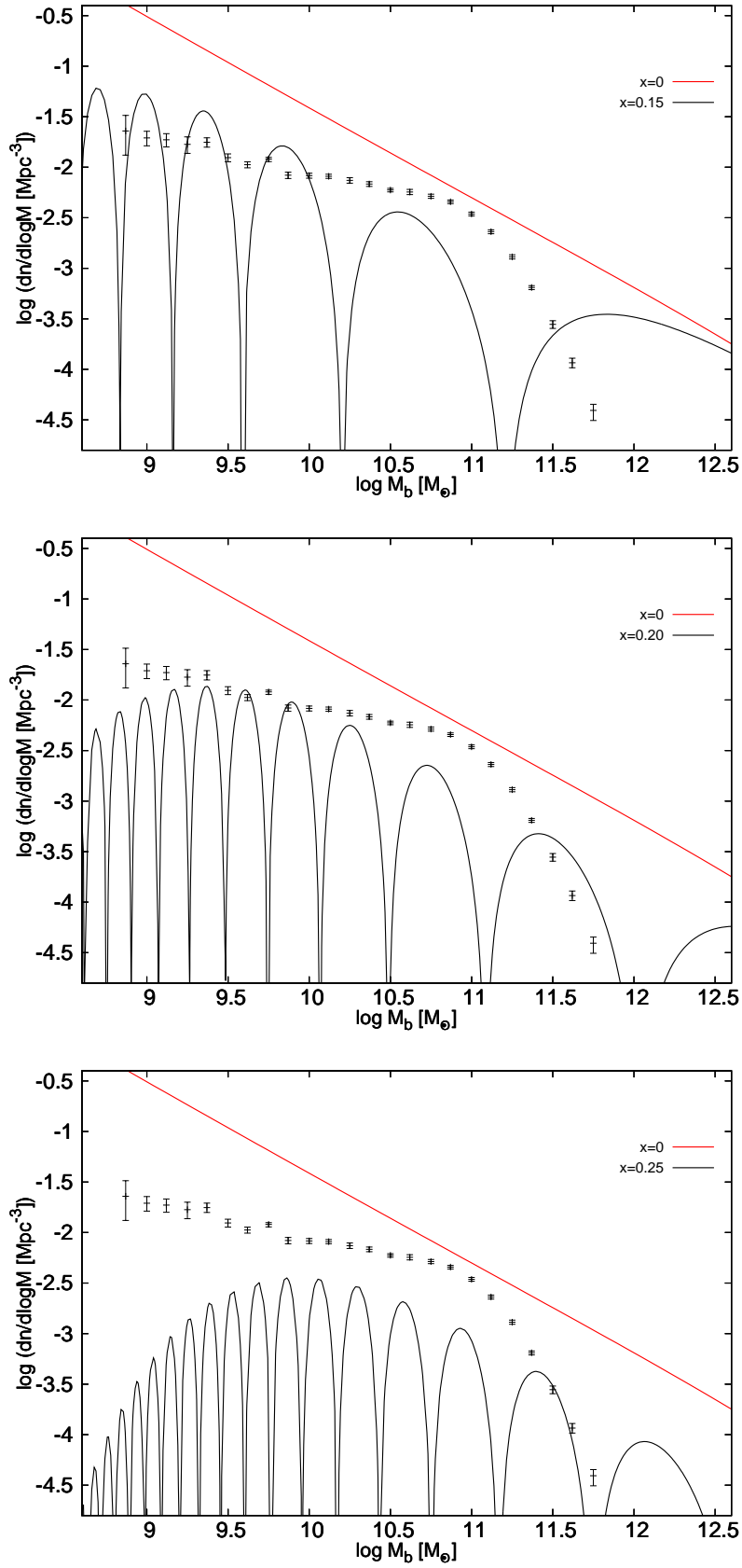
$$\frac{dn}{d \ln M_{\text{halo}}} = \frac{1}{12\pi^2} \frac{\bar{\rho}}{M_{\text{halo}}} \nu f(\nu) \frac{P(1/R)}{\delta_c^2 R^3} \, . \tag{10}$$

The sharp-k filter, unlike its real space counterpart, does not naturally have a mass scale M_{halo} associated to the filter scale R. This problem can be resolved by matching the expected analytic form for the halo mass function to simulations, which yields:

$$M_{\text{halo}} = \frac{4\pi\bar{\rho}}{3} (cR)^3 \, , \tag{11}$$

where $c \simeq 2.5$ [60,61]. We will use $c = 2.5$ in our numerical work.

Figures 2a,2b,2c: Halo mass function, $\log(dn/d\log M_{\text{halo}}\ [\text{Mpc}^{-3}])$ versus $\log[M_b/M_\odot]$ with $M_b = 0.15 M_{\text{halo}}$ for $x = 0$ (top red line, corresponding to $\epsilon = 0$) and $x = 0.15,\ 0.20,\ 0.25$ (corresponding to $\epsilon/10^{-10} \simeq 2.3,\ 4.2,\ 6.5$). Data is the galaxy stellar mass function from [90].

By using the linear power spectrum computed in the previous section we can use the EPS formalism with sharp-k filter to obtain the halo number density in terms of halo mass for the dissipative DM model of Section 2. We again consider mirror DM parameters and the fiducial cosmology as in Section 3. This serves as a useful estimate for mirror DM, as well as providing an illustrative example of the more generic dissipative case.

Given that the halo mass is difficult to measure, it is desirable to relate M_{halo} to a more directly observable quantity. The most readily observable quantities are connected to the luminous tracers of the DM halos, and this brings us to examine the luminosity and rotational velocity functions. We consider a simplified model where the baryon mass content of galaxies, M_b, is related to the halo mass by a simple proportionality relation. That is, $M_b \propto M_{\text{halo}}$, and we set the proportionality constant to the cosmic value, $\Omega_b/\Omega_m \simeq 0.15$. Such a high value for the baryon to halo mass ratio for spiral galaxies appears to be in some tension (by around a factor of two or three) with weak lensing studies and satellite kinematics (e.g. [65, 66]).[5] Naturally, these constraints on the M_b/M_{halo} ratio depend on the specific assumptions made such as the choice of DM halo profile and baryonic mass-to-light ratio, and of course the total mass of baryons in spiral galaxies is uncertain (see e.g. [93]). In any case variation of the M_b/M_{halo} ratio by a factor of 2 or 3 does not significantly affect our conclusions.

Figure 2 gives the results for the halo mass function $dn/d\log M_{\text{halo}}$ plotted against $M_b = 0.15 M_{\text{halo}}$. Notice that within our simplified model where $M_b \propto M_{\text{halo}}$, $d\log M_{\text{halo}} = d\log M_b$, and hence the results in Figure 2 are additionally a proxy for the baryonic mass function. The data in Figure 2 is the galaxy stellar mass function obtained from [90] (which also provides a rough estimate for baryons given that large galaxies are typically dominated by stars).

The oscillations apparent in Figure 2 are due to dark acoustic oscillations in the matter power spectrum. These DAOs are not diminished at all with the sharp-k filter, but would be expected to be diluted to some extent if a more physical filter could be found. Ultimately, detailed simulations should be used to quantify the true magnitude of the DAO effects that might be imprinted on the mass function.[6] The first few acoustic oscillations at the largest galaxy scales would present the best chance to detect dark acoustic oscillations. Actually, our results in Figure 2a and 2b suggest the intriguing possibility that the first dark acoustic oscillation might be connected (or at least contribute) to the downturn at $\log(M_b/M_\odot) \approx 11.2$ if $\epsilon \approx 3 \times 10^{-10}$. On smaller scales though, DAOs might be difficult to observe as they are expected to be largely smoothed out in the process of going from M_{halo} to M_b to observations. Also, nonlinear evolution (which is not accounted for in our linear Boltzmann treatment) would progressively erase DAOs, regenerating power on scales which were initially affected by them [50].

---

[5]However, we have checked that $M_b/M_{\text{halo}} \approx 0.15$ is roughly consistent (i.e. typically within no more than a factor of two) with inferences from rotation curves of specific galaxies. Taking the NGC 2903 spiral galaxy as an example, M_{halo} can be estimated from the fit to the rotation curve with quasi-isothermal profile [91] (the quasi-isothermal profile is roughly consistent with expectations assuming dissipative halo dynamics [35, 51, 57]). This gives a lower bound on M_{halo} because the radial extent of the halo is unknown. Taking the radial extent of the halo to be given by the largest radius for which rotation curve measurements are available, i.e. about 30 kpc for NGC 2903, gives the lower limit: $\log M_{\text{halo}}/M_\odot \gtrsim 11.4$. Combining this limit with the baryonic mass estimate $\log M_b/M_\odot \simeq 10.5$ [91], yields a rough limit $M_b/M_{\text{halo}} \lesssim 0.13$. Considering the gas rich dwarf DDO 154 as another example, a similar procedure using results from [92] gives the upper limit $M_b/M_{\text{halo}} \lesssim 0.10$.

[6] Some simulations of models featuring DAOs have been carried out in [50]. However, the effective halo mass resolution in those simulations would need to be improved by an order of magnitude or more if one wishes to investigate to full extent the impact of DAOs on the abundance of small galaxies.
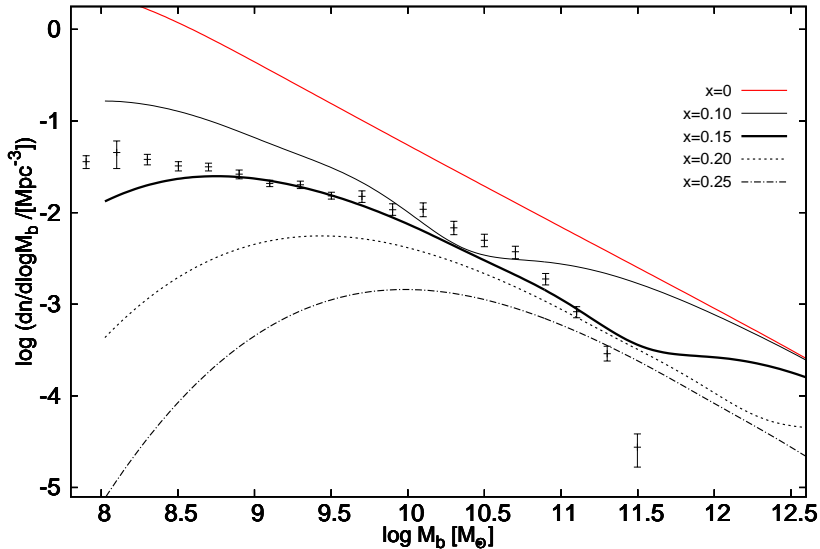
Figure 3: Baryonic mass function, $\log(dn/d\log M_b \ [\mathrm{Mpc}^{-3}])$, versus $\log(M_b/M_\odot)$, in the simplified model with $M_b = 0.15 M_{\mathrm{halo}}$. Curves top to bottom are for $x = 0$ (red curve) and $x = 0.10,\ 0.15,\ 0.20,\ 0.25$ (corresponding to $\epsilon/10^{-10} = 0,\ 1.04,\ 2.3,\ 4.2,\ 6.5$ respectively). Data is from [94].

For the purposes of the present paper, we shall model these anticipated smoothing effects in a phenomenological way by convolving the halo mass function with a Gaussian:

$$\frac{dn}{d\log M_b} \equiv \frac{1}{\sigma\sqrt{2\pi}} \int \frac{dn}{d\log M_{\mathrm{halo}}} \ e^{-0.5\{[\log(0.15\times M_{\mathrm{halo}})-\log(M_b)]/\sigma\}^2} \ d\log M_{\mathrm{halo}} \ . \qquad (12)$$

In Figure 3 we plot the baryonic mass function defined in this way, with $\sigma = 0.4$, compared with the galaxy baryonic mass function from [94]. The galaxy baryonic mass function includes the baryonic gas component which can dominate over stars for the smaller galaxies. The effect of varying σ is shown in Figure 4 for $x = 0.15$. This figure indicates that the effect of variation of the phenomenological parameter σ is rather modest, except perhaps at low σ where the oscillation effects start to become noticeable.

An alternative way of comparing the theory to observations is to use the galaxy velocity function rather than the baryonic mass function. That is, $dn/d\log V_c$, where V_c is the (circular) rotational velocity of the galaxy. This distribution can be estimated from the halo mass function using the baryonic Tully-Fisher relation to relate M_b to V_c:

$$\log[M_b/m_\odot] = s\log[V_c/(\mathrm{km/s})] + \log[A] \ . \qquad (13)$$

The quantities s and A were found in [95] to be $s = 3.75 \pm 0.11$ and $\log[A] = 2.18 \pm 0.23$ from a fit to a galaxy sample with accurate distance measurements (we use the central values of these quantities in our numerical work). Given the baryonic Tully-Fisher relation, the galaxy velocity function is simply:

$$\frac{dn}{d\log V_c} = s \ \frac{dn}{d\log M_b} \ . \qquad (14)$$

The velocity function defined in this way is shown in Figure 5 (for the same parameter set as per Figure 3).
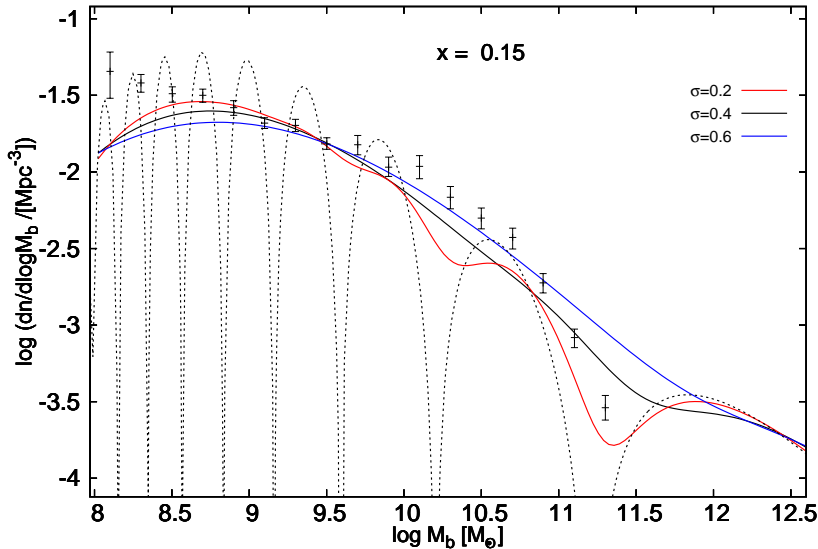
Figure 4: Baryonic mass function, $\log(dn/d\log M_b \ [\text{Mpc}^{-3}])$, versus $\log(M_b/M_\odot)$, in the simplified model with $M_b = 0.15 M_{\text{halo}}$ for $x = 0.15$ ($\epsilon \simeq 2.3 \times 10^{-10}$). Curves top to bottom are smoothed via Eq.(12) with $\sigma = 0.6$ (blue) $\sigma = 0.4$ (black) and $\sigma = 0.2$ (red). Also shown (dotted line) is the unsmoothed halo mass function. Data is from [94].

Also shown in Figure 5 is the measurement of the velocity function using data from the HI Parkes All Sky Survey (HIPASS) [13]. Although the theoretical curves give the mass function averaged over the Universe, the measurements in Figure 5 (as with Figure 3) can only provide the velocity function (mass function) for the smallest galaxies in the nearby region: $V \sim (5 \ \text{Mpc})^3$. Indeed, the effect of cosmic variance on the velocity function was examined in [13] by subdividing their sample into four quadrants. The resulting velocity function for each quadrant exhibited a factor of two variation in the normalization, the shape, however, was found to deviate significantly less.

In deriving the baryonic mass function in figures 3,4 one should keep in mind that the results depend significantly on the simple assumptions adopted, the most important of which is that $M_b \propto M_{\text{halo}}$. Of course, if there are baryonic physics processes that lead to gas outflows then this could possibly invalidate this simple assumption. In addition, dark baryonic physics processes could potentially also occur, especially at early times when dark star formation is envisaged. Notice that the baryonic mass function predicted in the $\epsilon = 0$ limit reduces to that of collisionless CDM, and even in that case it has been argued that inclusion of baryonic physics could result in a baryonic mass function in good agreement with observations, e.g [19, 20]. Obviously allowing for such large baryonic (and potentially also dark baryonic) physics effects could therefore lead to a wide range for the kinetic mixing parameter, ϵ. Nevertheless, the magnitude of the baryonic physics effects is rather uncertain, and might still be relatively minor, e.g. [16]. Indeed, direct observational evidence for large-scale gas outflows appears to be absent e.g. [96–101], although it is possible that large-scale gas outflows occur at early times when observations are currently limited. Even if large outflows occur, there remain serious challenges in reconciling the steep galaxy stellar mass function with observations of dwarf galaxies, e.g. [102, 103]. At any rate, if the baryonic effects do turn out to be minor, then the baryonic mass function would be a direct probe the dark sector physics, which is the optimistic case we have considered.
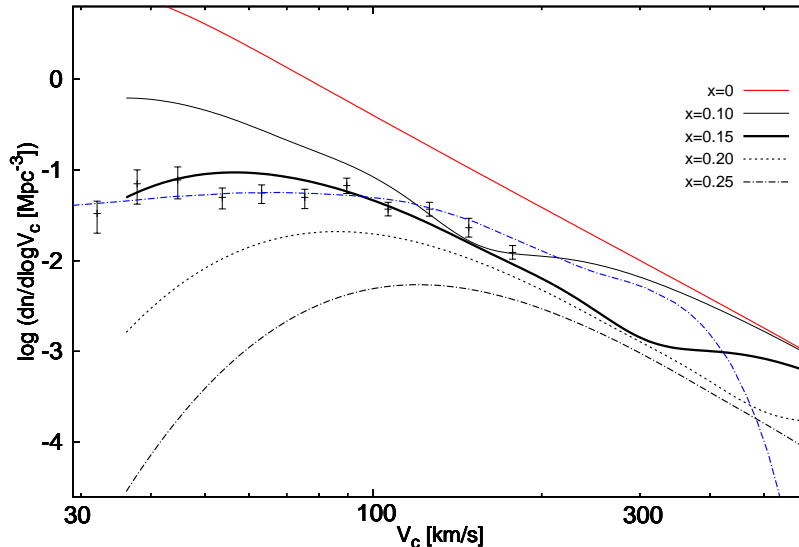
Figure 5: The velocity function $\log(dn/d\log V_c \,[\mathrm{Mpc}^{-3}])$ versus $V_c[\mathrm{km/s}]$ for dissipative dark matter. The top to bottom lines are for $x = 0$ (red) and $x = 0.10$, 0.15, 0.20, 0.25 (corresponding to $\epsilon/10^{-10} \simeq 0$, 1.04, 2.3, 4.2, 6.5 respectively). Data points are the HIPASS data for $V_c < 200$ km/s (gas rich sample), while the blue dashed dotted line is an estimate of the total galaxy count (i.e. including the most massive galaxies) [13].

Our results indicate that the considered dissipative DM model can provide a rough explanation of the shape and normalization of the measured galaxy luminosity and velocity functions. Furthermore, $x \approx 0.15$, that is, $\epsilon \approx 2 \times 10^{-10}$ [by Eq.(3)] is implicated for mirror DM parameters. This of course assumes that baryonic and dark baryonic physics do not play major roles in modifying the assumed $M_b \propto M_{\mathrm{halo}}$ scaling, which is an important caveat as discussed above. Allowing for the various uncertainties, suggests a preferred parameter range of roughly $x = 0.10 - 0.20$ or $\epsilon/10^{-10} = [1.0 - 4.2]$. Such ϵ values are consistent with the kinetic mixing strength required by the dynamical halo model of [30,51,55]. Recall that, in that picture, the halo takes the form of a dissipative plasma which evolves in response to various heating and cooling processes. At the current epoch DM halos around spiral and irregular galaxies are (typically) presumed to have reached a steady-state configuration where heating and cooling rates locally equilibrate. The heating is presumed to arise from ordinary core collapse supernovae, with kinetic mixing playing a critical role in converting a significant fraction of the supernova's core collapse energy into dark photons. In order for this heating to be dynamically important, $\epsilon \gtrsim 10^{-10}$ is required.

The number of large galaxies, i.e. with $M_b \gtrsim 2 \times 10^{11} \, M_\odot$, is observed to be exponentially suppressed. In the case of collisionless CDM this downturn is believed to be caused by inefficient cooling and energy injection from central super-massive black holes (see e.g. [104]). It is likely that these effects play a role in the dissipative DM case too. However, the results for $\sigma = 0.20$, $x = 0.15$ shown in Figure 4 suggest that it is possible that the first dark acoustic oscillation might also be connected with the dip at $\log(M_b/m_\odot) \approx 11.2$. More subtle dissipative DM effects could also contribute, e.g. if the halo cooling timescale were sufficiently long then it could slow the formation of such

large halos ($M_{\text{halo}} \gtrsim 10^{12} \ M_\odot$) and thereby affect the rate of large galaxy formation.[7]

At very low halo masses, $M_{\text{halo}} \lesssim 10^8 \ M_\odot$, power is exponentially cutoff due to diffusion damping (for mirror DM parameters). The number of very small galaxies is thereby expected to be strongly suppressed. The halo mass function gives the number of collapsed halo objects to be compared with field galaxies (or clusters on larger scales). Although we haven't explicitly calculated the number of satellites around a host (conditional mass function), it is clear that the number of satellites will also be strongly suppressed. In fact, the model can potentially "over solve" the missing satellite problem. However, the small satellites might have a very different history to field galaxies. Rather than evolving out of primordial density perturbations, small satellite galaxies might have formed more violently in a top-down process. In fact, we will argue below that if dark matter is dissipative then this provides a simple explanation for the observed planar and co-rotating distribution of satellite galaxies around the Milky Way [105], Andromeda [106] and possibly other hosts [107].

In dissipative DM models, a region with $\delta(\mathbf{x}; R) > \delta_c$ can undergo gravitational collapse and cool forming a dark disk. Baryons can also collapse, potentially forming a separate disk. Of course there can be some amount of baryons in the dark disk (and vice versa). In the model of [30, 51, 55], the dark disk is eventually heated, and any DM not within compact dark matter objects (dark stars) can thereby evolve to form the roughly spherical dark halo. Returning to early times though, when the more massive dark disk was forming, the complicated nonlinear collapse process is not expected to be uniform and perturbations near the edge of the disk could ultimately break off and provide the seeds of small satellite galaxies. Despite the complexity of this picture, it suggests a very simple explanation for the observed planar and co-rotating distribution of dwarf spheroidal galaxies around the Milky Way and Andromeda.[8] These satellites broke off from the dark disk which formed at very early times, thereby preserving this planar and co-rotating structure.[9] If they did indeed form in this way then there will be other ramifications. For example, they may have a much larger proportion of DM when compared with bottom-up forming galaxies.

---

[7]Another possibility, especially relevant for the mirror DM special case, is that the ionization state of the halo undergoes a transition at $M_{\text{halo}} \sim 10^{12} \ M_\odot$. In the mirror DM model, the halo contains mirror "metal" components possibly dominated by mirror oxygen. These metal components play a critical role in halo dynamics as their photoionization provides the mechanism for transferring supernovae core-collapse energy to the halo. However the mirror oxygen component is estimated to become fully ionized at $T_{\text{halo}} \approx 0.5$ keV which corresponds roughly to $M_{\text{halo}} \sim 10^{12} \ M_\odot$ given our assumed $M_b = 0.15 M_{\text{halo}}$ and the connection between T_{halo} and V_c in this model (see for instance [35]). This could result in a significant reduction in halo heating as photoionization becomes less effective at transferring the energy produced by ordinary supernovae to the halo. In the absence of sufficient heating the dissipative halo would contract perhaps triggering AGN activity and/or dark star formation, which might result in a limiting galaxy scale.

[8]One can further speculate that the observed polar orientation of the satellite planes with respect to the baryonic disk is a consequence of the nontrivial dynamics. Dark supernovae can be a powerful source of SM photons (due to the kinetic mixing interaction) which can heat the baryonic disk at early times providing a pressure force. While gravitational attraction between the two disks tend to make them merge (cf. [46]), the pressure force from the disk heating can work in the opposite manner and can potentially overwhelm the gravitational force. If this is the case, then the baryonic disk would be expected to evolve until it aligns with polar orientation.

[9]A related but still distinct possibility discussed in [108, 109] is that the satellites broke off from the baryonic disk as a result of an ancient merger event [110–112]. Galaxies produced in this way are known as tidal dwarf galaxies. At the present time though, it is unclear whether the dwarf spheroidal satellites of the Milky Way and Andromeda could be interpreted as tidal dwarf galaxies [113, 114].

5   Conclusion

In this paper, we have studied the abundance and clustering of small-scale structure in the context of dissipative dark matter models. Such models feature suppressed power on small scales due to acoustic damping and diffusion damping before and around the epoch of dark recombination. We estimated the damping scales analytically and initially studied their effect on the clustering of matter by computing the late-time matter power spectrum. Through this small-scale power suppression, these models have the potential to address the apparent deficit of nearby small galaxies, including the "missing satellite problem", as they naturally reduce the abundance of structure below the damping scales.

Subsequently, we explored the impact of the power suppression on the abundance of small-scale structure by using a variant of the extended Press-Schechter formalism. Within this formalism we estimated the halo mass function for the particular parameter set corresponding to mirror dark matter. This serves as a good estimate for mirror DM, as well as providing a useful example illustrating possibilities in more generic dissipative models. The halo mass function gives the number density of collapsed objects as a function of halo mass. Unfortunately, the halo mass itself is difficult to directly measure, so we considered the luminous tracers of the dark matter halos. To make contact with such observations, we considered a simplified model where $M_b \propto M_{\text{halo}}$, and set the proportionality constant to the cosmic value, $\Omega_b/\Omega_m \simeq 0.15$. This allowed us to connect the host halo mass to properties of its tracers such as luminosity or rotational velocity.

With mirror DM parameters set, the luminosity or rotational velocity functions depends only on one parameter: the kinetic mixing strength ϵ. Acoustic damping due to DAOs can supply moderate suppression of structure on galactic scales, which nevertheless is sufficient to yield a baryonic mass function which compares reasonably well with the observations, provided $\epsilon \approx 2 \times 10^{-10}$. This value of ϵ is consistent with the previously estimated range of ϵ favoured in dissipative halo dynamics: $\epsilon \gtrsim 10^{-10}$ [30, 51, 55]. Such a kinetic mixing strength also makes the model interesting for direct detection experiments which can probe dissipative DM via electron and nuclear recoils (e.g. [76] and references there-in). A particularly distinctive signature arises due to the capture of DM within the Earth. The consequent shielding of a detector from part of the halo DM wind results in a large diurnal modulation effect which is enhanced for a detector located in the Southern Hemisphere [74–76].

The predicted baryonic mass function falls much more steeply below the diffusion damping scale. For mirror DM parameters, this indicates that the abundance of very small galaxies, i.e. with $M_{\text{halo}} \lesssim 10^8 \ M_\odot$, is severely reduced. This in turn suggests a very different origin for the dwarf spheroidal satellite galaxies. They may have formed via a top-down process, as the result of nonlinear dissipative collapse of larger density perturbations. This origin might also explain some of their peculiar features, including the fact that they preferentially orbit in a planar distribution around their host (for the Milky Way and Andromeda systems). This plane should align with a remnant dark disk embedded in the dark halo of the host galaxy.

In the present work we computed the baryonic mass function at the present time (z=0). Future work could examine the redshift dependence of the observables we considered, which could easily be studied within the extended Press-Schechter formalism. Also, we have evaluated the abundance and clustering of small-scale structure for mirror dark matter parameters only. It should be straightforward to extend this study to more generic dissipative dark matter models, in particular examining the effects of the variation of all the fundamental parameters associated with the dissipative dark matter

model defined in Section 2. Understanding the properties of satellite galaxies seems to be a more difficult proposition if these very small galaxies are indeed formed from a top-down nonlinear fragmentation process. Presumably, a full understanding of this problem would require simulations to be performed. Finally, we emphasise again that direct detection experiments will provide the critical test for these models.

Appendix A - Damping scales

Here we provide approximate analytical expressions for the acoustic damping (DAO) and diffusion damping (dark Silk) scales.

A.1 - Acoustic damping scale

The acoustic damping scale is given by the sound horizon at the epoch of dark recombination:

$$L_{\mathrm{DAO}} \simeq \int_0^{\eta_{\mathrm{dr}}} d\eta \; c_D(\eta) = \int_{z_{\mathrm{dr}}}^{\infty} dz \; \frac{c_D(z)}{H(z)} \; . \tag{15}$$

Here η denotes conformal time $[d\eta \equiv dt/a(t)]$, z is the corresponding redshift, η_{dr} is the value of conformal time at dark recombination and $H(z)$ is the Hubble parameter. Also, c_D denotes the sound speed in the dark sector and is given by:

$$c_D(z) = \frac{1}{\sqrt{3}} \left[1 + \Delta(z) \right]^{-\frac{1}{2}} \; , \tag{16}$$

where:

$$\Delta(z) \equiv \frac{3\rho_{\mathrm{dm}}}{4\rho_{\gamma_D}} = \frac{B}{1+z} \; . \tag{17}$$

Here, $B \equiv 45\Omega_{\mathrm{dm}}\rho_{\mathrm{crit}}/(4\pi^2 x^4 T_0^4)$, $\rho_{\mathrm{crit}} \equiv 3H_0^2/(8\pi G)$ is the critical density, $T_0 \simeq 2.7256$ K is the current CMB temperature, and we have used $T_\gamma(z) = T_0(1+z)$. Also, the ratio between the temperatures in the two sectors, x, is given in Eq.(3).

The acoustic damping scale, Eq.(15), depends on the redshift of dark recombination, z_{dr}, which can be estimated in terms of the fundamental parameters of our model:

$$\frac{1}{1+z_{\mathrm{dr}}} = \frac{T_0}{T_{\mathrm{dr}}} = \frac{xT_0}{T'_{\mathrm{dr}}} \simeq \frac{2x\xi T_0}{\alpha_d^2 m_{e_d}} \; . \tag{18}$$

Here we have related the dark recombination temperature, T'_{dr}, to the $e_d(s)\text{-}p_d$ bound state binding energy $I' \approx \alpha_d^2 m_{e_d}/2$ by $T'_{\mathrm{dr}} = I'/\xi$. The parameter ξ depends only logarithmically on the fundamental parameters and was estimated to be $\xi \approx 40$ in [51].

The integral, Eq.(15) can be analytically solved. Using $H(z) = H_0(1+z)^2\sqrt{\Omega_r}$, appropriate for the radiation dominated era (the redshifts of interest satisfy $z \gtrsim z_{\mathrm{dr}} \gtrsim z_{\mathrm{eq}}$), we find:

$$L_{\mathrm{DAO}} = \frac{2}{H_0\sqrt{3\Omega_r B}} \left(\sqrt{1+y} - 1 \right) \; , \tag{19}$$

where:

$$y \equiv \frac{B}{z_{dr}+1} \approx 87 \left(\frac{10^{-9}}{\epsilon} \right)^{3/2} \left(\frac{\mathcal{M}}{m_e} \right)^{3/4} \left(\frac{\alpha}{\alpha_d} \right)^2 \left(\frac{m_e}{m_{e_d}} \right) \; . \tag{20}$$

Evidently, for a large range of parameter space, $y \gg 1$, and Eq.(19) reduces to:

$$L_{\mathrm{DAO}} \approx \frac{2}{H_0\sqrt{3\Omega_r B(z_{dr}+1)}}$$

$$\approx 8.6 \left(\frac{\epsilon}{10^{-9}}\right)^{5/4} \left(\frac{\alpha}{\alpha_d}\right) \left(\frac{m_e}{\mathcal{M}}\right)^{5/8} \left(\frac{m_e}{m_{e_d}}\right)^{1/2} h^{-1} \, \mathrm{Mpc} \, . \qquad (21)$$

The corresponding associated comoving wavenumber is $k_{\mathrm{DAO}} \approx \pi/L_{\mathrm{DAO}}$, and one can easily check that it is consistent with our numerical results shown in Figures 1, 2.

A.2 - Diffusion damping scale

On scales below the dark photon mean free path, dark diffusion damping is efficient in erasing the DM fluctuations. The physics is virtually identical to the well studied case of photon diffusion. Following standard arguments (e.g. [115]), the diffusion scale, L_{DSD}, can be estimated to be:

$$L_{\mathrm{DSD}} \approx \pi \left[\int_0^{\eta_{\mathrm{dr}}} d\eta' \, \frac{1}{6(1+\Delta)n_{e_d}\sigma_{T_d}a(\eta')} \left(\frac{\Delta^2}{1+\Delta} + \frac{8}{9}\right) \right]^{\frac{1}{2}} , \qquad (22)$$

where $\sigma_{T_d} = 8\pi\alpha_d^2/(3m_{e_d}^2)$ is the dark Thomson cross-section. This integral evaluates to:

$$L_{\mathrm{DSD}} \approx \pi \left[\frac{m_{p_d}}{18 H_0 \sqrt{\Omega_r}\Omega_{\mathrm{dm}}(1+z_{\mathrm{dr}})^3\rho_{\mathrm{crit}}\sigma_{T_d}} \right]^{\frac{1}{2}} , \qquad (23)$$

where we have made the assumption that $m_{e_d} \ll m_{p_d}$. Using Eqs.(3,18), L_{DSD} can be expressed in terms of the fundamental parameters:

$$L_{\mathrm{DSD}} \approx 0.7 \left(\frac{\epsilon}{10^{-9}}\right)^{3/4} \left(\frac{\alpha}{\alpha_d}\right)^4 \left(\frac{m_e}{\mathcal{M}}\right)^{3/8} \left(\frac{m_e}{m_{e_d}}\right)^{1/2} \left(\frac{m_{p_d}}{m_p}\right)^{\frac{1}{2}} h^{-1} \, \mathrm{Mpc} \, . \qquad (24)$$

For mirror DM parameters, $L_{\mathrm{DSD}} < L_{\mathrm{DAO}}$, however more generally, $L_{\mathrm{DSD}} > L_{\mathrm{DAO}}$ is possible. The associated comoving wavenumber is $k_{\mathrm{DSD}} \approx \pi/L_{\mathrm{DSD}}$, and like k_{DAO} is also consistent with our numerical results shown in Figures 1,2.

The length scales L_{DAO} and L_{DSD} and corresponding comoving wavenumber scales are derived in linear perturbation theory (i.e. prior to the nonlinear collapse phase). The mass scales that correspond to these length scales are roughly: $M_{\mathrm{DAO}} \sim \pi\rho_{\mathrm{crit}}\Omega_m L_{\mathrm{DAO}}^3/6$, $M_{\mathrm{DSD}} \sim \pi\rho_{\mathrm{crit}}\Omega_m L_{\mathrm{DSD}}^3/6$. In terms of the wavenumber, k, the correspondence is approximately [from Eq.(11)]:

$$M(k) \approx 3 \times 10^{12} \left(\frac{k}{\mathrm{Mpc}^{-1}}\right)^{-3} M_\odot \, . \qquad (25)$$

Acknowledgments

References

[1] P. A. R. Ade *et al.*, "Planck 2015 results. XIII. Cosmological parameters," *arXiv: 1502.01589*, 2015.

[2] R. Keisler *et al.*, "A Measurement of the Damping Tail of the Cosmic Microwave Background Power Spectrum with the South Pole Telescope," *Astrophys. J.*, vol. 743, p. 28, 2011.

[3] G. Hinshaw *et al.*, "Nine-Year Wilkinson Microwave Anisotropy Probe (WMAP) Observations: Cosmological Parameter Results," *Astrophys. J. Suppl.*, vol. 208, p. 19, 2013.

[4] M. Tegmark *et al.*, "The 3-D power spectrum of galaxies from the SDSS," *Astrophys. J.*, vol. 606, pp. 702–740, 2004.

[5] S. Cole *et al.*, "The 2dF Galaxy Redshift Survey: Power-spectrum analysis of the final dataset and cosmological implications," *Mon. Not. Roy. Astron. Soc.*, vol. 362, pp. 505–534, 2005.

[6] C. Blake *et al.*, "The WiggleZ Dark Energy Survey: mapping the distance-redshift relation with baryon acoustic oscillations," *Mon. Not. Roy. Astron. Soc.*, vol. 418, pp. 1707–1724, 2011.

[7] C. P. Ahn *et al.*, "The Ninth Data Release of the Sloan Digital Sky Survey: First Spectroscopic Data from the SDSS-III Baryon Oscillation Spectroscopic Survey," *Astrophys. J. Suppl.*, vol. 203, p. 21, 2012.

[8] L. Anderson *et al.*, "The clustering of galaxies in the SDSS-III Baryon Oscillation Spectroscopic Survey: Baryon Acoustic Oscillations in the Data Release 9 Spectroscopic Galaxy Sample," *Mon. Not. Roy. Astron. Soc.*, vol. 427, no. 4, pp. 3435–3467, 2013.

[9] K. S. Dawson *et al.*, "The Baryon Oscillation Spectroscopic Survey of SDSS-III," *Astron. J.*, vol. 145, p. 10, 2013.

[10] W. J. G. de Blok, "The Core-Cusp Problem," *Adv. Astron.*, vol. 2010, p. 789293, 2010.

[11] A. A. Klypin, A. V. Kravtsov, O. Valenzuela, and F. Prada, "Where are the missing Galactic satellites?," *Astrophys. J.*, vol. 522, pp. 82–92, 1999.

[12] B. Moore *et al.*, "Dark matter substructure within galactic halos," *Astrophys. J.*, vol. 524, pp. L19–L22, 1999.

[13] M. A. Zwaan, M. J. Meyer, and L. Staveley-Smith, "The velocity function of gas-rich galaxies," *Mon. Not. Roy. Astron. Soc.*, vol. 403, p. 1969, 2010.

[14] A. Klypin, I. Karachentsev, D. Makarov, and O. Nasonova, "Abundance of Field Galaxies," *Mon. Not. Roy. Astron. Soc.*, vol. 454, p. 1798, 2015.

[15] E. Papastergis, R. Giovanelli, M. P. Haynes, and F. Shankar, "Is there a ?too big to fail? problem in the field?," *Astron. Astrophys.*, vol. 574, p. A113, 2015.

[16] J. Zavala *et al.*, "The velocity function in the local environment from LCDM and LWDM constrained simulations," *Astrophys. J.*, vol. 700, pp. 1779–1793, 2009.

[17] M. Boylan-Kolchin, J. S. Bullock, and M. Kaplinghat, "Too big to fail? The puzzling darkness of massive Milky Way subhaloes," *Mon. Not. Roy. Astron. Soc.*, vol. 415, p. L40, 2011.

[18] D. H. Weinberg *et al.*, "Cold dark matter: controversies on small scales," in *Sackler Colloquium: Dark Matter Universe: On the Threshhold of Discovery Irvine, USA, October 18-20, 2012*, 2013.

[19] M. Vogelsberger *et al.*, "Introducing the Illustris Project: Simulating the coevolution of dark and visible matter in the Universe," *Mon. Not. Roy. Astron. Soc.*, vol. 444, no. 2, pp. 1518–1547, 2014.

[20] J. Schaye *et al.*, "The EAGLE project: Simulating the evolution and assembly of galaxies and their environments," *Mon. Not. Roy. Astron. Soc.*, vol. 446, pp. 521–554, 2015.

[21] B. Moore, "Evidence against dissipationless dark matter from observations of galaxy haloes," *Nature*, vol. 370, p. 629, 1994.

[22] D. N. Spergel and P. J. Steinhardt, "Observational evidence for selfinteracting cold dark matter," *Phys. Rev. Lett.*, vol. 84, pp. 3760–3763, 2000.

[23] R. Foot, "Mirror matter-type dark matter," *Int. J. Mod. Phys.*, vol. D13, pp. 2161–2192, 2004.

[24] S. I. Blinnikov and M. Khlopov, "Possible astronomical effects of mirror particles," *Sov. Astron.*, vol. 27, pp. 371–375, 1983. [Astron. Zh.60,632(1983)].

[25] H. M. Hodges, "Mirror baryons as the dark matter," *Phys. Rev.*, vol. D47, pp. 456–459, 1993.

[26] R. Foot, H. Lew, and R. R. Volkas, "A Model with fundamental improper space-time symmetries," *Phys. Lett.*, vol. B272, pp. 67–70, 1991.

[27] Z. Berezhiani, D. Comelli, and F. L. Villante, "The Early mirror universe: Inflation, baryogenesis, nucleosynthesis and dark matter," *Phys. Lett.*, vol. B503, pp. 362–375, 2001.

[28] A. Yu. Ignatiev and R. R. Volkas, "Mirror dark matter and large scale structure," *Phys. Rev.*, vol. D68, p. 023518, 2003.

[29] Z. Berezhiani, P. Ciarcelluti, D. Comelli, and F. L. Villante, "Structure formation with mirror dark matter: CMB and LSS," *Int. J. Mod. Phys.*, vol. D14, pp. 107–120, 2005.

[30] R. Foot and R. R. Volkas, "Spheroidal galactic halos and mirror dark matter," *Phys. Rev.*, vol. D70, p. 123508, 2004.

[31] R. Foot and Z. K. Silagadze, "Supernova explosions, 511-keV photons, gamma ray bursts and mirror matter," *Int. J. Mod. Phys.*, vol. D14, pp. 143–152, 2005.

[32] P. Ciarcelluti, "Cosmology with mirror dark matter," *Int. J. Mod. Phys.*, vol. D19, pp. 2151–2230, 2010.

[33] R. Foot, "Implications of mirror dark matter kinetic mixing for CMB anisotropies," *Phys. Lett.*, vol. B718, pp. 745–751, 2013.

[34] P. Ciarcelluti and Q. Wallemacq, "Is dark matter made of mirror matter? Evidence from cosmological data," *Phys. Lett.*, vol. B729, pp. 62–66, 2014.

[35] R. Foot, "Mirror dark matter: Cosmology, galaxy structure and direct detection," *Int. J. Mod. Phys.*, vol. A29, p. 1430013, 2014.

[36] H. Goldberg and L. J. Hall, "A New Candidate for Dark Matter," *Phys. Lett.*, vol. B174, p. 151, 1986.

[37] Z. G. Berezhiani, A. D. Dolgov, and R. N. Mohapatra, "Asymmetric inflationary reheating and the nature of mirror universe," *Phys. Lett.*, vol. B375, pp. 26–36, 1996.

[38] A. Ibarra, A. Ringwald, and C. Weniger, "Hidden gauginos of an unbroken U(1): Cosmological constraints and phenomenological prospects," *JCAP*, vol. 0901, p. 003, 2009.

[39] L. Ackerman, M. R. Buckley, S. M. Carroll, and M. Kamionkowski, "Dark Matter and Dark Radiation," *Phys. Rev.*, vol. D79, p. 023519, 2009.

[40] J. L. Feng, M. Kaplinghat, H. Tu, and H.-B. Yu, "Hidden Charged Dark Matter," *JCAP*, vol. 0907, p. 004, 2009.

[41] D. E. Kaplan, G. Z. Krnjaic, K. R. Rehermann, and C. M. Wells, "Atomic Dark Matter," *JCAP*, vol. 1005, p. 021, 2010.

[42] S. Andreas, M. D. Goodsell, and A. Ringwald, "Dark matter and dark forces from a supersymmetric hidden sector," *Phys. Rev.*, vol. D87, no. 2, p. 025007, 2013.

[43] J.-W. Cui, H.-J. He, L.-C. Lu, and F.-R. Yin, "Spontaneous Mirror Parity Violation, Common Origin of Matter and Dark Matter, and the LHC Signatures," *Phys. Rev.*, vol. D85, p. 096003, 2012.

[44] J. M. Cline, Z. Liu, and W. Xue, "Millicharged Atomic Dark Matter," *Phys. Rev.*, vol. D85, p. 101302, 2012.

[45] F.-Y. Cyr-Racine and K. Sigurdson, "Cosmology of atomic dark matter," *Phys. Rev.*, vol. D87, no. 10, p. 103515, 2013.

[46] J. Fan, A. Katz, L. Randall, and M. Reece, "Double-Disk Dark Matter," *Phys. Dark Univ.*, vol. 2, pp. 139–156, 2013.

[47] F.-Y. Cyr-Racine, R. de Putter, A. Raccanelli, and K. Sigurdson, "Constraints on Large-Scale Dark Acoustic Oscillations from Cosmology," *Phys. Rev.*, vol. D89, no. 6, p. 063517, 2014.

[48] T. Banks, W. Fischler, D. Lorshbough, and W. Tangarife, "Implications Of A Dark Sector U(1) For Gamma Ray Bursts," *Phys. Rev.*, vol. D90, no. 4, p. 043538, 2014.

[49] K. Petraki, L. Pearce, and A. Kusenko, "Self-interacting asymmetric dark matter coupled to a light massive dark photon," *JCAP*, vol. 1407, p. 039, 2014.

[50] M. R. Buckley *et al.*, "Scattering, Damping, and Acoustic Oscillations: Simulating the Structure of Dark Matter Halos with Relativistic Force Carriers," *Phys. Rev.*, vol. D90, no. 4, p. 043524, 2014.

[51] R. Foot and S. Vagnozzi, "Dissipative hidden sector dark matter," *Phys. Rev.*, vol. D91, p. 023512, 2015.

[52] L. Pearce, K. Petraki, and A. Kusenko, "Signals from dark atom formation in halos," *Phys. Rev.*, vol. D91, p. 083532, 2015.

[53] M. Heikinheimo, M. Raidal, C. Spethmann, and H. Veermäe, "Dark matter self-interactions via collisionless shocks in cluster mergers," *Phys. Lett.*, vol. B749, pp. 236–241, 2015.

[54] M. Reece and T. Roxlo, "Nonthermal production of dark radiation and dark matter," *arXiv:1511.06768*, 2015.

[55] R. Foot, "Galactic structure explained with dissipative mirror dark matter," *Phys. Rev.*, vol. D88, no. 2, p. 023520, 2013.

[56] R. Foot, "Tully-Fisher relation, galactic rotation curves and dissipative mirror dark matter," *JCAP*, vol. 1412, no. 12, p. 047, 2014.

[57] R. Foot, "Dissipative dark matter explains rotation curves," *Phys. Rev.*, vol. D91, no. 12, p. 123543, 2015.

[58] R. Foot, "Dissipative dark matter and the rotation curves of dwarf galaxies," *arXiv: 1506.01451*, 2015.

[59] A. J. Benson *et al.*, "Dark Matter Halo Merger Histories Beyond Cold Dark Matter: I - Methods and Application to Warm Dark Matter," *Mon. Not. Roy. Astron. Soc.*, vol. 428, p. 1774, 2013.

[60] A. Schneider, R. E. Smith, and D. Reed, "Halo Mass Function and the Free Streaming Scale," *Mon. Not. Roy. Astron. Soc.*, vol. 433, p. 1573, 2013.

[61] A. Schneider, "Structure formation with suppressed small-scale perturbations," *Mon. Not. Roy. Astron. Soc.*, vol. 451, no. 3, pp. 3117–3130, 2015.

[62] W. H. Press and P. Schechter, "Formation of galaxies and clusters of galaxies by self-similar gravitational condensation," *Astrophys. J.*, vol. 187, pp. 425–438, 1974.

[63] J. R. Bond, S. Cole, G. Efstathiou, and N. Kaiser, "Excursion set mass functions for hierarchical Gaussian fluctuations," *Astrophys. J.*, vol. 379, p. 440, 1991.

[64] J. S. Bullock, A. V. Kravtsov, and D. H. Weinberg, "Reionization and the abundance of galactic satellites," *Astrophys. J.*, vol. 539, p. 517, 2000.

[65] A. A. Dutton *et al.*, "The Kinematic Connection Between Galaxies and Dark Matter Haloes," *Mon. Not. Roy. Astron. Soc.*, vol. 407, pp. 2–16, 2010.

[66] R. Mandelbaum, "Galaxy Halo Masses from Weak Gravitational Lensing," *IAU Symp.*, vol. 311, pp. 86–95, 2015.

[67] K. Petraki and R. R. Volkas, "Review of asymmetric dark matter," *Int. J. Mod. Phys.*, vol. A28, p. 1330028, 2013.

[68] K. M. Zurek, "Asymmetric Dark Matter: Theories, Signatures, and Constraints," *Phys. Rept.*, vol. 537, pp. 91–121, 2014.

[69] R. Foot and X.-G. He, "Comment on Z Z-prime mixing in extended gauge theories," *Phys. Lett.*, vol. B267, pp. 509–512, 1991.

[70] B. Holdom, "Two U(1)'s and Epsilon Charge Shifts," *Phys. Lett.*, vol. B166, p. 196, 1986.

[71] E. D. Carlson and S. L. Glashow, "Nucleosynthesis Versus the Mirror Universe," *Phys. Lett.*, vol. B193, p. 168, 1987.

[72] R. Foot, "Mirror dark matter cosmology - predictions for $N_{eff}[CMB]$ and $N_{eff}[BBN]$," *Phys. Lett.*, vol. B711, pp. 238–243, 2012.

[73] H. Vogel and J. Redondo, "Dark Radiation constraints on minicharged particles in models with a hidden photon," *JCAP*, vol. 1402, p. 029, 2014.

[74] R. Foot, "Diurnal modulation due to self-interacting mirror and hidden sector dark matter," *JCAP*, vol. 1204, p. 014, 2012.

[75] R. Foot and S. Vagnozzi, "Diurnal modulation signal from dissipative hidden sector dark matter," *Phys. Lett.*, vol. B748, pp. 61–66, 2015.

[76] J. D. Clarke and R. Foot, "Plasma dark matter direct detection," *JCAP*, vol. 1601, no. 01, p. 029, 2016.

[77] K. Petraki, M. Trodden, and R. R. Volkas, "Visible and dark matter from a first-order phase transition in a baryon-symmetric universe," *JCAP*, vol. 1202, p. 044, 2012.

[78] P. Ciarcelluti and R. Foot, "Primordial He' abundance implied by the mirror dark matter interpretation of the DAMA/Libra signal," *Phys. Lett.*, vol. B690, pp. 462–465, 2010.

[79] I. M. Shoemaker, "Constraints on Dark Matter Protohalos in Effective Theories and Neutrinophilic Dark Matter," *Phys. Dark Univ.*, vol. 2, no. 3, pp. 157–162, 2013.

[80] M. Escudero *et al.*, "Exploring dark matter microphysics with galaxy surveys," *JCAP*, vol. 1509, no. 09, p. 034, 2015.

[81] C. Bœhm *et al.*, "Using the Milky Way satellites to study interactions between cold dark matter and radiation," *Mon. Not. Roy. Astron. Soc.*, vol. 445, pp. L31–L35, 2014.

[82] J. A. Schewtschenko *et al.*, "Dark matter–radiation interactions: the impact on dark matter haloes," *Mon. Not. Roy. Astron. Soc.*, vol. 449, no. 4, pp. 3587–3596, 2015.

[83] J. Silk, "Cosmic black body radiation and galaxy formation," *Astrophys. J.*, vol. 151, pp. 459–471, 1968.

[84] M. Zaldarriaga, L. Hui, and M. Tegmark, "Constraints from the Lyman alpha forest power spectrum," *Astrophys. J.*, vol. 557, pp. 519–526, 2001.

[85] P. McDonald *et al.*, "The Lyman-alpha forest power spectrum from the Sloan Digital Sky Survey," *Astrophys. J. Suppl.*, vol. 163, pp. 80–109, 2006.

[86] U. Seljak, A. Makarov, P. McDonald, and H. Trac, "Can sterile neutrinos be the dark matter?," *Phys. Rev. Lett.*, vol. 97, p. 191303, 2006.

[87] S. Bird, H. V. Peiris, M. Viel, and L. Verde, "Minimally Parametric Power Spectrum Reconstruction from the Lyman-alpha Forest," *Mon. Not. Roy. Astron. Soc.*, vol. 413, pp. 1717–1728, 2011.

[88] A. R. Zentner, "The Excursion Set Theory of Halo Mass Functions, Halo Clustering, and Halo Growth," *Int. J. Mod. Phys.*, vol. D16, pp. 763–816, 2007.

[89] R. K. Sheth, H. J. Mo, and G. Tormen, "Ellipsoidal collapse and an improved model for the number and spatial distribution of dark matter haloes," *Mon. Not. Roy. Astron. Soc.*, vol. 323, p. 1, 2001.

[90] E. F. Bell, D. H. McIntosh, N. Katz, and M. D. Weinberg, "The optical and near-infrared properties of galaxies. 1. Luminosity and stellar mass functions," *Astrophys. J. Suppl.*, vol. 149, p. 289, 2003.

[91] W. J. G. de Blok *et al.*, "High-Resolution Rotation Curves and Galaxy Mass Models from THINGS," *Astron. J.*, vol. 136, pp. 2648–2719, 2008.

[92] S.-H. Oh *et al.*, "High-resolution mass models of dwarf galaxies from LITTLE THINGS," *Astron. J.*, vol. 149, p. 180, 2015.

[93] M. Longhetti and P. Saracco, "Stellar mass estimates in early-type galaxies: procedures, uncertainties and models dependence," *Mon. Not. Roy. Astron. Soc.*, vol. 394, p. 774, 2009.

[94] E. Papastergis *et al.*, "A direct measurement of the baryonic mass function of galaxies & implications for the galactic baryon fraction," *Astrophys. J.*, vol. 759, p. 138, 2012.

[95] F. Lelli, S. S. McGaugh, and J. Schombert, "The small scatter of the baryonic Tully-Fisher relation," *arXiv:1512.04543*, 2015.

[96] C. L. Martin, "The impact of star formation on the interstellar medium in dwarf galaxies. 2. The formation of galactic winds," *Astrophys. J.*, vol. 506, pp. 222–252, 1998.

[97] J. van Eymeren, D. J. Bomans, K. Weis, and R. J. Dettmar, "Outflow or galactic wind: The fate of ionized gas in the halos of dwarf galaxies," *Astron. Astrophys.*, 2007. [Astron. Astrophys.474,67(2007)].

[98] J. van Eymeren *et al.*, "A kinematic study of the irregular dwarf galaxy NGC 2366 using HI and Halpha observations," *Astron. Astrophys.*, vol. 493, p. 511, 2009.

[99] F. Lelli, F. Fraternali, and M. Verheijen, "Evolution of dwarf galaxies: a dynamical perspective," *Astron. Astrophys.*, vol. 563, p. A27, 2014.

[100] F. Lelli, M. Verheijen, and F. Fraternali, "Dynamics of starbursting dwarf galaxies," *Astron. Astrophys.*, vol. 566, p. A71, 2014.

[101] H. Katz *et al.*, "Testing Feedback-Modified Dark Matter Haloes with Galaxy Rotation Curves: Estimation of Halo Parameters and Consistency with ΛCDM," *arXiv:1605.05971*, 2016.

[102] I. Ferrero *et al.*, "The dark matter halos of dwarf galaxies: a challenge for the LCDM paradigm?," *Mon. Not. Roy. Astron. Soc.*, vol. 425, pp. 2817–2823, 2012.

[103] J. Penarrubia, A. Pontzen, M. G. Walker, and S. E. Koposov, "The coupling between the core/cusp and missing satellite problems," *Astrophys. J.*, vol. 759, p. L42, 2012.

[104] D. J. Croton *et al.*, "The Many lives of AGN: Cooling flows, black holes and the luminosities and colours of galaxies," *Mon. Not. Roy. Astron. Soc.*, vol. 365, pp. 11–28, 2006. [Erratum: Mon. Not. Roy. Astron. Soc.367,864(2006)].

[105] M. S. Pawlowski, J. Pflamm-Altenburg, and P. Kroupa, "The VPOS: a vast polar structure of satellite galaxies, globular clusters and streams around the Milky Way," *Mon. Not. Roy. Astron. Soc.*, vol. 423, p. 1109, 2012.

[106] R. A. Ibata *et al.*, "A Vast Thin Plane of Co-rotating Dwarf Galaxies Orbiting the Andromeda Galaxy," *Nature*, vol. 493, pp. 62–65, 2013.

[107] N. G. Ibata, R. A. Ibata, B. Famaey, and G. F. Lewis, "Velocity anti-correlation of diametrically opposed galaxy satellites in the low redshift universe," *Nature*, vol. 511, p. 563, 2014.

[108] R. Foot and Z. K. Silagadze, "Thin disk of co-rotating dwarfs: A fingerprint of dissipative (mirror) dark matter?," *Phys. Dark Univ.*, vol. 2, pp. 163–165, 2013.

[109] L. Randall and J. Scholtz, "Dissipative Dark Matter and the Andromeda Plane of Satellites," *JCAP*, vol. 1509, no. 09, p. 057, 2015.

[110] F. Hammer *et al.*, "Does M31 result from an ancient major merger?," *Astrophys. J.*, vol. 725, pp. 542–555, 2010.

[111] S. Fouquet *et al.*, "Does the dwarf galaxy system of the Milky Way originate from Andromeda?," *Mon. Not. Roy. Astron. Soc.*, vol. 427, p. 1769, 2012.

[112] Y. Yang *et al.*, "Reproducing properties of MW dSphs as descendants of DM-free TDGs," *Mon. Not. Roy. Astron. Soc.*, vol. 442, p. 2419, 2014.

[113] F. Lelli *et al.*, "Gas dynamics in tidal dwarf galaxies: disc formation at z=0," *Astron. Astrophys.*, vol. 584, p. A113, 2015.

[114] H. Flores *et al.*, "Young tidal dwarf galaxies cannot be used to probe dark matter in galaxies," *Mon. Not. Roy. Astron. Soc.*, vol. 457, p. 14, 2015.

[115] S. Dodelson, *Modern Cosmology.* Amsterdam: Academic Press, 2003.